AIAA JOURNAL
Vol. 34, No. 10, October 1996

Modified Trajectory Method for Practical Global Optimization Problems

A. A. Groenwold,* J. A. Snyman,† and N. Stander‡
University of Pretoria, Pretoria 0002, South Africa

A modification of the Snyman–Fatti (SF) stochastic multistart trajectory method for global optimization is developed. In the modified SF algorithm, distinction is made between a global and a local phase in the application of the original minimization procedure for a particular starting point. The global phase ensures convergence to the neighborhood of a relative low local minimum, whereas in the local phase further accuracy is pursued. Different choices of parameter values are proposed for the individual phases, and a procedure is proposed to deal with simple bound violations. The modifications lead to substantial improvement in the efficiency of the original trajectory method. The performance of the modified algorithm is assessed by its application to a selection of test problems and the results are compared with those of some other methods. The method is also successfully applied to laminate structural problems in which optimal sequences of the ply orientations of the layers are determined.

Introduction

THE problem of globally optimizing a real valued function is inherently intractable (unless hard restrictions are imposed on the objective function) in that no practically useful characterization of the global optimum is available. Indeed the problem of determining an accurate estimate of the global optimum is mathematically ill-posed in the sense that very similar objective functions may have global optima very distant from each other.[1] Nevertheless, the need in practice to find a relative low local minimum has resulted in considerable research over the last decade to develop algorithms that attempt to find such a low minimum. For a very good and comprehensive survey of global optimization, the reader is referred to the work of Törn and Zilinkas.[2]

Two distinct approaches to global optimization have been identified, namely deterministic and stochastic methods. The first class are those algorithms that implicitly search all of the function domain and thus are guaranteed to find the global optimum. The algorithms within this class are forced to deal with severely restricted classes of functions (e.g., Lipschitz continuous functions with known Lipschitz constants). Even with these restrictions it is often computationally infeasible to apply deterministic algorithms to search for the guaranteed global optimum as the number of computations required increases exponentially with the dimension of the feasible space. To overcome the inherent difficulties of the guaranteed-accuracy algorithms, much research effort has been devoted to algorithms in which a stochastic element is introduced; this way the deterministic guarantee is relaxed into a confidence measure. The best performing algorithms for global optimization are in fact found within the class of stochastic algorithms. A general stochastic algorithm for global optimization consists of three major steps[1]: a sampling step, an optimization step, and a check of some stopping criterion. This paper is concerned with such an algorithm and in particular with the modification of the algorithm to substantially improve its efficiency.

The algorithm to be modified is the multistart trajectory method of Snyman and Fatti.[3] This algorithm, hereafter referred to as the SF algorithm, is philosophically similar to the simulated annealing technique (see survey by Schoen[1]) in the sense that it also corresponds to the simulation of a physical process, in particular the dynamic trajectory of a particle under the influence of a potential force. The algorithm also contains heuristic and probabilistic elements. The trajectory allows the particle to skip over locally stable (minimum energy) configurations as occurs in simulated annealing. The method also has similarities to the trajectory method of Aluffi-Pentini et al.[4] in which paths of a stochastic-differential equation are computed.

The SF algorithm has been shown to be competitive with other global optimization methods when applied to standard test problems.[3] It has also been used by Kam and Snyman[5] to investigate the lamination arrangements of laminated composite plates. In these problems where many local optima occur, the algorithm proved reliable and effective in producing the global optimum designs.

In spite of the reported successes of the SF algorithm it remains an extremely expensive method. In this paper modifications are presented to improve the efficiency of the method. The improvements are demonstrated by assessing the performance of the modified algorithm in comparison with the performance of some recently evaluated global optimization methods[6] on a selection of standard test functions. The practicality of the modified algorithm is further supported by its successful application to the optimization of some nontrivial orthotropic membrane, plate, and shell structures with respect to ply-angle sequence.

Before dealing with the modifications to the SF algorithm, it is necessary to clearly introduce the basic methodology of the Snyman and Fatti trajectory approach to the global optimization problem.

SF Trajectory Method

The general global optimization problem may be formulated as follows. Given a real valued objective function $f(\boldsymbol{x})$ defined on the set $\boldsymbol{x} \in D$ in $\mathbb{R}^n$, find the point $\boldsymbol{x}^*$ and the corresponding function value f^* such that

$$f^* = f(\boldsymbol{x}^*) = \text{minimum}\,\{f(\boldsymbol{x}) \mid \boldsymbol{x} \in D\} \tag{1}$$

if such a point $\boldsymbol{x}^*$ exists. If the objective function and/or the feasible domain D are nonconvex, then there may be many local minima that are not global.

If D corresponds to all $\mathbb{R}^n$, the optimization problem is unconstrained. Even in this case simple bounds are imposed in practice so that effectively an almost unconstrained problem is considered with D corresponding to the hyper box defined by

$$D = \{\boldsymbol{x} \mid \boldsymbol{l} \leq \boldsymbol{x} \leq \boldsymbol{u}\} \tag{2}$$

where $\boldsymbol{l}$ and $\boldsymbol{u}$ are n vectors defining the respective lower and upper bounds on $\boldsymbol{x}$. The term D is sometimes also referred to as the domain or region of interest.

Received April 13, 1995; revision received April 4, 1996; accepted for publication April 8, 1996.

*Graduate Research Assistant, Structural and Multidisciplinary Optimization Research Group, Department of Mechanical and Aeronautical Engineering.

†Professor, Structural and Multidisciplinary Optimization Research Group, Department of Mechanical and Aeronautical Engineering.

‡Professor, Structural and Multidisciplinary Optimization Research Group, Department of Mechanical and Aeronautical Engineering. Member AIAA.

The essentials of the original SF algorithm[3] using dynamic search trajectories for unconstrained global minimization will now be discussed. For more details concerning the motivation of the method, its detailed construction, convergence theorems, computational aspects, and some of the more obscure heuristics employed, the reader is referred to the original paper.

Dynamic Trajectories

In the SF algorithm successive sample points $\boldsymbol{x}^j$, $j = 1, 2, \ldots$, are selected at random from the box D defined by Eq. (2). For each sample point $\boldsymbol{x}^j$, a sequence of trajectories T^i, $i = 1, 2, \ldots$, is computed by numerically solving the successive initial value problems

$$\ddot{\boldsymbol{x}}(t) = -\nabla f[\boldsymbol{x}(t)] \qquad \boldsymbol{x}(0) = \boldsymbol{x}_0^i; \qquad \dot{\boldsymbol{x}}(0) = \dot{\boldsymbol{x}}_0^i \tag{3}$$

This trajectory represents the motion of a particle of unit mass in an n-dimensional conservative force field, where the function to be minimized represents the potential energy.

Trajectory T^i is terminated when $\boldsymbol{x}(t)$ reaches a point where $f[\boldsymbol{x}(t)]$ is arbitrarily close to the value $f(\boldsymbol{x}_0^i)$ while moving uphill or, more precisely, if $\boldsymbol{x}(t)$ satisfies the conditions

$$f[\boldsymbol{x}(t)] > f(\boldsymbol{x}_0^i) - \epsilon_u \qquad \dot{\boldsymbol{x}}(t)^T \nabla f[\boldsymbol{x}(t)] > 0 \tag{4}$$

where ϵ_u is an arbitrary small prescribed positive value.

An argument is presented in Ref. 3 to show that provided the level set $\{\boldsymbol{x} \mid f(\boldsymbol{x}) \leq f(\boldsymbol{x}_0^i)\}$ is bounded and $\nabla f(\boldsymbol{x}_0^i) \neq 0$, then conditions of Eq. (4) will be satisfied at some finite point in time.

Each computed step along trajectory T^i is monitored so that at termination the point $\boldsymbol{x}_m^i$ at which the minimum value was achieved is recorded together with the associated velocity $\dot{\boldsymbol{x}}_m^i$ and function value f_m^i. The values of $\boldsymbol{x}_m^i$ and $\dot{\boldsymbol{x}}_m^i$ are used to determine the initial values for the next trajectory T^{i+1}. From a comparison of the minimum values, the best point $\boldsymbol{x}_b^i$ for the current j over all trajectories to date is also recorded. In more detail the minimization procedure for a given sample point $\boldsymbol{x}^j$, in computing the sequence $\boldsymbol{x}_b^i$, $i = 1, 2, \ldots$, is as follows.

Minimization Procedure (MP)

1) For given sample point $\boldsymbol{x}^j$, set $\boldsymbol{x}_0^1 := \boldsymbol{x}^j$ and compute T^1 subject to $\dot{\boldsymbol{x}}_0^1 := 0$; record $\boldsymbol{x}_m^1$, $\dot{\boldsymbol{x}}_m^1$, and f_m^1; set $\boldsymbol{x}_b^1 := \boldsymbol{x}_m^1$ and $i := 2$.

2) Compute trajectory T^i with $\boldsymbol{x}_0^i := \frac{1}{2}(\boldsymbol{x}_0^{i-1} + \boldsymbol{x}_b^{i-1})$ and $\dot{\boldsymbol{x}}_0^i := \frac{1}{2}\dot{\boldsymbol{x}}_m^{i-1}$; record $\boldsymbol{x}_m^i$, $\dot{\boldsymbol{x}}_m^i$, and f_m^i.

3) If $f_m^i < f(\boldsymbol{x}_b^{i-1})$, then $\boldsymbol{x}_b^i := \boldsymbol{x}_m^i$; else $\boldsymbol{x}_b^i := \boldsymbol{x}_b^{i-1}$.

4) Set $i := i + 1$ and go to 2.

In the original paper[3] an argument is presented to indicate that under normal conditions on the continuity of f and its derivatives, $\boldsymbol{x}_b^i$ will converge to a local minimum. Procedure MP, for a given j, is accordingly terminated at preceding steps if $\|\nabla f(\boldsymbol{x}_b^i)\| \leq \epsilon$, for some small prescribed positive value ϵ, and $\boldsymbol{x}_b^i$ is taken as the local minimizer $\boldsymbol{x}_f^j$; i.e., set $\boldsymbol{x}_f^j := \boldsymbol{x}_b^i$ with corresponding function value $f_f^j := f(\boldsymbol{x}_f^j)$.

Reflecting on the overall approach just outlined, involving the computation of energy conserving trajectories and the minimization procedure, it should be evident that, in the presence of many local minima, the probability of convergence to a relative low local minimum is increased. This one expects because, with a small value of ϵ_u [see conditions (4)], it is likely that the particle will move through a trough associated with a relative high local minimum and move over a ridge to record a lower function value at a point beyond. Since we assume that the level set associated with the starting point function is bounded, termination of the search trajectory will occur as the particle eventually moves to a region of higher function values.

Define the region of convergence of the preceding method for a local minimum $\hat{\boldsymbol{x}}$ as the set of all points $\boldsymbol{x}$ that, used as starting points for the preceding procedure, converges to $\hat{\boldsymbol{x}}$. One may reasonably expect that in the case where the regions of attraction (for the usual gradient-descent methods, see Ref. 7) of the local minima are more or less equal, the region of convergence of the global minimum will be relatively increased.

Global Stopping Criterion

The preceding method requires a termination rule for deciding when to end the sampling and to take the current overall minimum function value $\tilde{f}$, i.e.,

$$\tilde{f} = \text{minimum}\left\{f_f^j, \text{ over all } j \text{ to date}\right\} \tag{5}$$

as the global minimum value f^*. The stopping criterion adopted in Ref. 3 is now briefly discussed.

Let R_k denote the region of convergence for the preceding MP procedure of local minimum $\hat{\boldsymbol{x}}^k$ and let α_k be the associated probability that a sample point be selected in R_k. The region of convergence and the associated probability for the global minimum $\boldsymbol{x}^*$ are denoted by R^* and α^*, respectively. The following basic assumption, which is probably true for many functions of practical interest, is now made.

A. Basic assumption: $\alpha^* \geq \alpha_k$ for all local minima $\hat{\boldsymbol{x}}^k$.

The following theorem may be proved.

B. Theorem[3]: Let r be the number of sample points falling within the region of convergence of the current overall minimum $\tilde{f}$ after $\tilde{n}$ points have been sampled. Then under assumption A and a statistically noninformative prior distribution the probability that $\tilde{f}$ corresponds to f^* may be obtained from

$$Pr[\tilde{f} = f^*] \geq q(\tilde{n}, r) = 1 - \frac{(\tilde{n}+1)!(2\tilde{n}-r)!}{(2\tilde{n}+1)!(\tilde{n}-r)!} \tag{6}$$

On the basis of this theorem this stopping rule was adopted: stop when $Pr[\tilde{f} = f^*] \geq q^*$, where q^* is some prescribed desired confidence level, typically chosen as 0.99.

Numerical Considerations

Because problem (3) is solved numerically, the computed trajectory $\boldsymbol{x}(t)$ is indeed not a continuous path but is represented by discrete points along the trajectory, computed at time intervals of length Δt used by the numerical integration scheme. For economy the simple Euler-forward Euler-backward (leap-frog)[3] method is used in which an initial choice for the time step $\Delta t := \Delta t_0$ is prescribed. This step is successively halved, if necessary to ensure descent on the first computed step.

A second consideration is the choice of ϵ_u to be used in Eq. (4) in terminating a trajectory. In practice it is extremely difficult to estimate what a good choice would be. On reflection a reasonable alternative to Eq. (4) is to terminate on the uphill once

$$f[\boldsymbol{x}(t)] - f_T \geq \alpha\left[f(\boldsymbol{x}_0^i) - f_T\right] \tag{7}$$

where α is a parameter chosen approximately equal to but less than 1 and f_T is an estimate of f^*. This is equivalent to the choice

$$\epsilon_u = (1-\alpha)\left[f(\boldsymbol{x}_0^i) - f_T\right] \tag{8}$$

If it is known that $f^* = 0$, as may often be the case, then there is no problem. Otherwise, successfully better estimates f_T to f^* are obtained from one computed trajectory to the other. In the original implementation $\alpha = 0.95$ was used.

Finally, because exact numerical convergence to a local minimum is not possible, a positive tolerance ω must be prescribed to decide whether or not an approximate local minimum value f_f^j reached corresponds to the current overall minimum $\tilde{f}$ [see Eq. (6)]. Accordingly, if

$$\left|f_f^j - \tilde{f}\right| < \omega \tag{9}$$

then it is assumed that the same overall minimum value $\tilde{f}$ has been reached.

The choice of the parameters ϵ, q^*, Δt_0, α, and ω introduced here play important roles in the efficiency and reliability of the trajectory method.

Modifications to the SF Algorithm

Although the SF algorithm has been proved to be as efficient as many other available methods, it is still extremely expensive. In general, for any global optimization algorithm it is desirable 1) to minimize the number of function and gradient evaluations without impairing performance with regard to a) accuracy and b) probability of finding the global optimum and 2) to minimize the computational effort associated with identifying nonoptimal local minima.

Obviously, the aforementioned should be done without prior knowledge of the objective function f. In an attempt to improve the efficiency of the SF algorithm with regard to computational effort, a number of modifications have been applied to the original algorithm. To explain these modifications it is necessary to distinguish now between a global and a local phase of the application of minimization procedure MP (see previous section) for a given sample point $\boldsymbol{x}^j$.

Global Phase

In this phase the procedure MP in which, for a given sample point, a sequence of trajectories is generated, is considered to have converged only if for l successive trajectories the condition $\|\nabla f\| < \epsilon_c$ is satisfied at k consecutive computed steps of each of the trajectories, at which point the particular trajectory is also terminated. The choice $k = 4, l = 3$, and $\epsilon_c = 2\epsilon$, where ϵ is the prescribed convergence parameter for the local phase to discussed later, was applied to all test functions used in this study.

After completion of the global phase, the computation for the current sample point $\boldsymbol{x}^j$ is stopped if

$$f_f^j > \tilde{f} = r\omega \tag{10}$$

where ω is the resolution tolerance defined by Eq. (9). If condition (10) is not satisfied, then greater accuracy is sought in the local phase. Here the value $r = 2$ is used.

Local Phase

In this phase, following on the global phase, the computation of further successive trajectories is continued until at any computed trajectory point the condition $\|\nabla f\| < \epsilon$ is satisfied. The choice $\epsilon = 10^{-4}$ was used throughout.

The insistence on values for k and l of greater than 1 in the global phase is to prevent the fortuitous and early termination in the neighborhood of a relative high local minimum and thus increases the probability of convergence to a comparative low local minimum. Stopping the computation prematurely if condition (10) is satisfied prevents unnecessarily accurate determination of nonoptimal local minima.

Influence of Parameter α

A further modification involves the choice of the value for α. In the global phase the originally proposed high value of $\alpha = 0.95$ is still used, which allows for the likelihood of the particle moving over a relative high ridge to a lower function value beyond. However, once convergence to the neighborhood of a local minimum has been established in the global phase, and only higher accuracy is sought in the local phase, it is no longer necessary to use a large value for α since such a choice would only unnecessarily lengthen the computed trajectories. Accordingly the choice $\alpha = 0.15$ is proposed and used in the local phase.

Adjustment of the Integration Time Step Δt

It was found that convergence to the higher accuracy $\|\nabla f\| < \epsilon$ occurs very slowly during the local phase. Because it can be shown that the increase in the physical step size along the trajectory is given by $\|\nabla f\| \Delta t^2$ and because both $\|\nabla f\|$ and Δt may be small at the start of the local phase, the steps during this phase may remain excessively small, resulting in uneconomical slow convergence. It is therefore proposed to systematically increase the time step Δt during the local phase. Here the time step Δt of the leap-frog integrating scheme is increased from one step to the next along the trajectory by setting $\Delta t := (1 + \mu)\Delta t$, where currently the choice $\mu = 0.1\Delta t_0$ is used and Δt_0 denotes the initial choice for Δt at the starting sample point and is also now used as the initial time step for each trajectory in the local phase. The adjustment described here for the local phase is not applied during the global phase.

Table 1 Griewank G1 function ($n = 2$): relative cost of analyses

	SF	PTT	SF-M
Success rate	6/26	6/26	6/26
NFE	3147	2315	2076
Relative cost	1.52	1.12	1.00

Table 2 Griewank G2 function ($n = 10$): relative cost of analyses

	SF	PTT	SF-M
Success rate	6/71	6/71	6/71
NFE	29,431	22,775	16,448
Relative cost	1.79	1.38	1.00

Violation of Simple Bounds

A further modification is applied once a trajectory exceeds a simple bound. In this case the component of the position vector $\boldsymbol{x}(t)$ that violates the bound is regenerated in a random fashion to lie within the region of interest D [see Eq. (2)]. The effect of this modification on a number of test problems is dramatic.

As an initial test of the overall influence of the modifications on the performance of the trajectory method, the modified method, hereafter referred to as the SF-M algorithm, was applied to the challenging Griewank functions[8] G1 and G2, and the results are presented in Tables 1 and 2, respectively. The term NFE denotes the number of function evaluations required. The success rates $r/\tilde{n}$ [see Eq. (6)] are also tested. The Griewank functions are trying indeed: G1 has some 500 local minima in the region of interest, and G2 has a few thousand. The number of variables is 2 and 10 for G1 and G2, respectively. The values used for the parameters are as specified earlier except for the initial time steps, which were taken as $\Delta t_0 = 2$ and 5 for G1 and G2, respectively.

The effect as a result of premature termination of the sequence of trajectories (PTT), which is the result of the application of condition (10) alone, is highly beneficial as is apparent from the separate entries in the tables for this case. As one may expect, the benefit increases when the success rate decreases (more nonoptimal local minima) because less computational effort is wasted on the accurate determination of the nonoptimal local minima. The results for the overall modified SF-M algorithm are listed in the last column showing a further significant reduction in computational cost.

Comparison with Other Techniques

The performance of the modified SF-M algorithm on a selection of standard test problems is now compared with that given for some other global optimization methods in a recently published evaluation by El-wakeil and Arora [Optimal Design Laboratory (ODL)].[6] They considered the following methods.

1) Evtushenko's Covering Method (Cov): The method belongs to the exact deterministic class, and it is assumed that the objective function satisfies a Lipschitz condition with known Lipschitz constant L. As L is, in general, not known, L is estimated by the method. Two versions are employed, namely Cov1, which has both local and global phases, and Cov2, which only has a global phase.

2) Acceptance-Rejection Method (A-R): The method has a statistical basis and is stochastic in nature. For this method no stopping criteria are available, and in the reported evaluation the search was simply terminated once the reported global minimum was within a specified tolerance of the known global optimum.

3) Controlled Random Search (CRS): The method is based on a simplex local search algorithm and employs 13^{n+1} random starting points, with n the number of variables.

In most practical applications the economy of a method is determined by the number of function evaluations required for convergence since the time required to step through the logic of the optimization routine is usually insignificant compared with the time

Table 3 Number of function evaluations for the standard test functions

Method	Test function				
	ODL.B1–1	ODL.B2–7	ODL.B2–8	ODL.B2–28	ODL.B6–29
Cov1	272	12,420	$>10^6$	$>10^6$	757
Cov2	199	917,413	$>10^6$	Not found	$>10^6$
A-R	24	48	287	249	2336
CRS	N/A	540	887	567	9446
SF	315	395	6263	974	5385
SF-M	242	294	5348	547	766
SF-M†	48	74	891	137	153

for the function evaluation. The methods are therefore compared with respect to the number of function evaluations, and the results are as listed in Table 3.

The test functions are classified as follows: the number of variables is indicated by n in the sequence ODL.Bn–m, with m a serial number. The functions all have relatively few local minima, except ODL.B2–8, which has 760 minima in the region of interest. However, there are 18 global optima, making this problem less trying than G1. ODL.B6–29 has the highest number of variables employed in the set of El-wakeil and Arora, namely 6. Results for ODL.B6–29 include the effect of random regeneration of infeasible vectors. In applying the SF-M algorithm the same parameter settings were used as for the Griewank functions, with the exception of the initial times step, which was always taken as $\Delta t_0 = 1$.

Comparison between the various methods is difficult, as no information about the probability to which the global optimization is calculated is presented for the methods in Ref. 11. In Table 3 a reasonable comparison is attempted by the following. For the SF-M method the number of function evaluations required to obtain a probability of 0.99 of convergence to the global optimum is divided by the number of successes [r in Eq. (6)]. These results are entered in the row denoted SF-M†. Each number, representing the average number of function evaluations per success, allows for a more reasonable comparison of the SF-M method with other methods that employ no stopping criteria.

Furthermore, the results obtained with the SF-M algorithm were calculated to a higher accuracy ($\epsilon = 10^{-4}$) than those of the other methods, which particularly for the test functions that terminate quickly is expensive and puts the SF-M algorithm at a disadvantage.

Although not conclusive, a comparison between the results for the SF-M and the A-R methods in Table 3 suggests that the SF-M algorithm requires fewer function evaluations to reach the global optimum for functions with either a large number of variables or a large number of local minima in the region of interest. In addition the results clearly show that the Cov1, Cov2, and CRS methods are not competitive. Furthermore, the absence of a suitable stopping criterion for the A-R method effectively disqualifies this method.

Optimal Design of Orthotropic Structures

It is desired to find the optimum lamination arrangement and number of layers for membrane, plate, or generally curved shell structures of given thickness. Minimization of the strain energy U, which is equivalent to the criterion of maximum stiffness, is selected as the objective function. Both symmetric and unsymmetric layered structures are considered.

Being a global optimization problem, U has many local minima $\hat{U}_j$ and corresponding local minimizers $\hat{\boldsymbol{\theta}}_j$, where $\boldsymbol{\theta}$ is the vector of ply orientations, which is explicitly given by $\boldsymbol{\theta} = (\theta_1, \theta_2, \ldots, \theta_{NL})^T$, with NL the number of layers. For symmetric ply layups, the number of variables is halved, giving $\boldsymbol{\theta} = (\theta_1, \theta_2, \ldots, \theta_{NL/2})_s^T$.

In mathematical form the optimization problem is written as follows:

Minimize

$$U(\boldsymbol{\theta}) \tag{11}$$

subject to

$$-90 \leq \theta_i \leq 90 \text{ deg}, \qquad i = 1, 2, \ldots, NL \tag{12}$$

Because the strain energy U is periodic with respect to $\boldsymbol{\theta}$, constraint equations (12) are implicitly satisfied, and an optimal $\boldsymbol{\theta}$ can be found by solving an unconstrained minimization problem.

The finite element method (FEM) is employed to discretize the structures, using the flat QC5D-SA shell element.[9,10] Denoting the assembled structural stiffness matrix as $\boldsymbol{K}$ and the nodal displacements as $\boldsymbol{q}$, the strain energy U of an assembled three-dimensional structure modeled with the QC5D-SA element is written as[11]

$$U = \tfrac{1}{2}\boldsymbol{q}^T\boldsymbol{K}\boldsymbol{q} \tag{13}$$

where the quantities $\boldsymbol{K}$ and $\boldsymbol{q}$ act in the global coordinate system and include the effect of membrane, bending, transverse shear and coupled membrane-bending actions. The unknowns $\boldsymbol{q}$ are obtained by solution of the governing equilibrium equations

$$\boldsymbol{K}\boldsymbol{q} = \boldsymbol{f} \tag{14}$$

where $\boldsymbol{f}$ indicates the consistent nodal loads. Considering only linear elastic structures, the derivatives of strain energy with respect to ply orientations in the global system are given by

$$\frac{\partial U}{\partial \theta_k} = -\frac{1}{2}\boldsymbol{q}^T\frac{\partial \boldsymbol{K}}{\partial \theta_k}\boldsymbol{q} \tag{15}$$

where $k = 1, 2, \ldots, NL$ for unsymmetric layups and $k = 1, 2, \ldots, NL/2$ for symmetric layups.

Numerical Results

In this section some numerical solutions for some general test problems are presented to illustrate the capabilities of the method. Exhaustive details of benchmarking of the shell element employed in the finite element analyses may be found in Refs. 9–11.

Simply Supported Centrally Loaded Plates

Consider a T300/5208 graphite/epoxy material, for which the Young's moduli, the shear modulus, and Poisson's ratio, respectively, are defined by[12] $E_{11}/E_0 = 181.0$, $E_{22}/E_0 = 10.3$, $G_{12}/E_0 = 7.17$, while $\nu_{12} = 0.28$ and $E_0 = 1.0$ GPa. In the following, P indicates a central point load, t is the plate thickness, and a and b indicate side lengths of the plates (Fig. 1). All layers are of equal thickness.

To enable comparison with series solution results, the plates are modeled as being symmetric and shear rigid. Shear rigidity is approximated through manipulation of the finite element shear correction factors. Results are reported in terms of the normalized plate center deflection $\bar{w}_c$ normalized as

$$\bar{w}_c = \frac{w_c \times 10^3}{Pb^3/E_0 at^3} \tag{16}$$

Tables 4 and 5 present the optimum results for plates with aspect ratios of 1.0 and 0.5, respectively. For the series solution results, the number of terms was always taken as 25 × 25, whereas the FEM mesh was taken as 16 × 16. Further mesh refinement is not performed. The number of layers (NL) is increased from 4 to 16, and complete global searches are performed for each arrangement. Clearly, very little is to be gained beyond eight layers.

In Table 4 note that for the 16-layered plate modeled with the FEM, the orientation of the two layers facing the element reference plane is irrelevant. Both a 45- and a −45-ply angle are allowable, as the contribution of these layers at both these angles towards the internal strain energy of the plate is almost negligible.

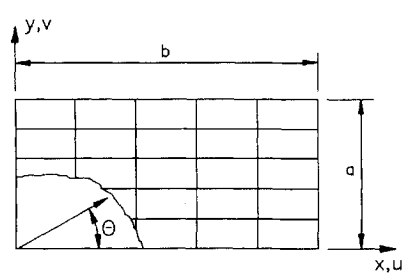

Fig. 1 Simply supported centrally loaded plates.

Table 4 Optimum ply arrangement for a simply supported, shear rigid plate under a central point load (b/a = 0.5)

	FEM results		Series solution	
NL	$\bar{w}_c$	θ_i^*	$\bar{w}_c$	θ_i^*
4	1.925	$[45.00/-45.00]_s$	1.915	$[45.00/-45.00]_s$
6	1.594	$[45.00/-45.00_2]_s$	1.593	$[45.00/-45.00_2]_s$
8	1.517	$[45.00/-45.00_3]_s$	1.513	$[45.00/-45.00_3]_s$
16	1.499	$[45.00/-45.00/45.00/-45.00_4/\pm 45.00]_s$	1.501	$[45.00/-45.00/45.00/-45.00_5]_s$

Table 5 Optimum ply arrangement for a simply supported, shear rigid plate under a central point load (b/a = 0.5)

	FEM results		Series solution	
NL	$\bar{w}_c$	θ_i^*	$\bar{w}_c$	θ_i^*
4	4.704	$[-4.49/56.86]_s$	4.750	$[-8.42/-55.49]_s$
6	4.386	$[18.84/-39.17/-39.10]_s$	4.414	$[19.52/-39.02/-39.05]_s$
8	4.274	$[26.17/-32.70_2/-32.89]_s$	4.298	$[26.54/-32.83_2/-32.81]_s$
16	4.252	$[29.59/-29.59_2/29.58/-29.60/29.48/29.58/-30.17]_s$	4.278	$[30.27/-29.35_2/30.26/-29.36/30.35/29.76/-29.83]_s$

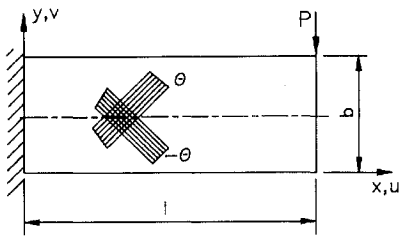

Fig. 2 Membrane cantilever.

Membrane Cantilever Under Transverse Shear

Depicted in Fig. 2, this problem was analyzed by Lakshminarayana and Murthy[13] for a number of discrete ply arrangements and an aspect ratio of $l/b = 40.0$ (unit thickness). Here, the effect of aspect ratio on optimum ply arrangement is studied. A 1×4 mesh employing QC5D-SA elements adequately discretizes the beam.[11] To prevent the appearance of undesirable twisting modes, symmetric QC5D-SA elements only are used. The material constants are $E_{11} = 30 \times 10^6$, $E_{22} = 7.5 \times 10^5$, $G_{12} = 4.5 \times 10^5$, and $\nu_{12} = 0.28$, whereas the transverse tip load $P = 10$.

Numerical results are presented in Table 6 for aspect ratios of $l/b = 40.0, 20, 10, 5$, and 2.5. For the most slender aspect ratio ($l/b = 40$) the effect of transverse shear is negligible. Therefore, longitudinal fibers carry the transverse tip load efficiently in pure bending and, as expected, the global optimum was always found at $\theta^* = [0.00_{NL/2}]_s$. Table 6 reveals that the effect of in-plane shear is not very pronounced for the aspect ratios of $l/b = 20$ and 10, although the effect for the latter might be slightly more than expected. For the lower aspect ratios the advantage of designing for in-plane shear is clearly illustrated in the table. Very little is to be gained by further increasing the number of layers (not shown in tabulated form).

Clamped Open Crown Hemispherical Shell

This doubly curved orthotropic shell example (Fig. 3) is from Moser and Schmid.[14] Two discrete single-ply arrangements are considered in Ref. 14, namely 0 deg (latitudinal) and 90 deg (longitudinal). Here, the shell is optimized with respect to both ply arrangements and number of layers. Both symmetric and unsymmetric ply arrangements are considered. As symmetry is lost, the shell is modeled in full. The material constants and geometry are defined by $E_{11} = 7.5 \times 10^6$, $E_{22} = 2 \times 10^6$, $G_{12} = 1.25 \times 10^6$, $\nu_{12} = 0.25$, and $\nu_{23} = 0.45$, whereas $P = 2$, $t = 1$, and $R = 100$.

The optimum ply arrangements, calculated with a graded 4×16 mesh to a probability of 0.99, are presented in Table 7. The layers are all of equal thickness. For the symmetric case, the six-layered shell can be taken as the optimum. For the unsymmetric case, the four-layered shell may be taken as the optimum.

Table 6 Membrane cantilever: optimum ply arrangement

l/b	NL	U^*	θ_i^*
40	2	4.243534	$[0.00]_s$
	4	4.243534	$[0.00/0.00]_s$
20	2	0.54678	$[0.00]_s$
	4	0.54669	$[1.45/-1.45]_s$
10	2	0.076520	$[0.00]_s$
	4	0.073922	$[6.53/-6.53]_s$
5	2	0.013664	$[0.000]_s$
	4	0.010696	$[11.44/-11.44]_s$
2.5	2	0.0037702	$[0.00]_s$
	4	0.0016942	$[18.26/-18.26]_s$

Table 7 Clamped open crown hemispherical shell: optimum ply arrangement

	U^*		
NL	Symmetric	Unsymmetric	θ_i^*
2	1.0011	——	$[0.00]_s$
2	——	1.0011	[0.00/0.00]
4	0.9533	——	$[8.66/-48.12]_s$
4	——	0.9356	[−6.56/48.47/−60.55/0.63]
6	0.9380	——	$[4.21/-32.53/59.37]_s$
6	——	0.9328	[5.59/−29.52/52.03/−72.08/−11.79/3.49]
8	0.9317	——	$[-1.09/5.95/-45.82/61.35]_s$
8	——	0.9305	[4.29/−16.97/41.23/−54.17/−71.82/50.48/−1.43/−2.68]
16	0.9314	——	$[-2.05/2.39/10.05/-7.9/-39.30/49.41/56.12/-72.09]_s$

The unsymmetric layup converges much more rapidly than the symmetric layup, although no differences are noted for a two-layered shell. Clearly, once convergence is reached, there is no practical difference between the symmetric and unsymmetric ply arrangements. However, by taking advantage of the unsymmetric formulation, the optimum stiffness is obtained at a lower number of layers, implying a potential cost saving as a result of the unsymmetric layup.

The example illustrates that, as was noted for the rectangular plates, also for shells, for both symmetric and unsymmetric layups, very little gain in maximum stiffness can be achieved beyond eight layers.

Pretwisted Beam

Utilizing the excellent performance of the flat QC5D-SA shell element for warped geometries,[11] this problem was devised to illustrate

Table 8 Optimum ply arrangement for the pretwisted beam

	Symmetric			
	Load case 1		Load case 2	
NL	$U^* \times 1000$	θ_i^*	$U^* \times 1000$	θ_i^*
2	1.2049	$[47.76]_s$	1.233	$[90.00]_s$
3	0.6811	$[45.70/\overline{-46.11}]_s$	1.227	$[89.59/\overline{-79.00}]_s$
4	0.4346	$[45.96/-46.43]_s$	1.226	$[89.64/-87.50]_s$
5	0.3604	$[46.18/-46.05/\overline{-61.60}]_s$	—	—
6	0.3313	$[46.43/-45.81/-53.40]_s$	—	—
8	0.3105	$[46.58/-45.88/-47.95/-74.37]_s$	—	—
	Unsymmetric			
	Load case 1		Load case 2	
NL	$U^* \times 1000$	θ_i^*	$U^* \times 1000$	θ_i^*
2	0.3087	[−46.76/46.76]	1.226	[90.00/−90.00]
3	0.3078	[−45.77/−61.50/46.61]	1.224	[90.42/78.82/−89.59]
4	0.3081	[−46.01/51.81/−51.81/46.01]	—	—

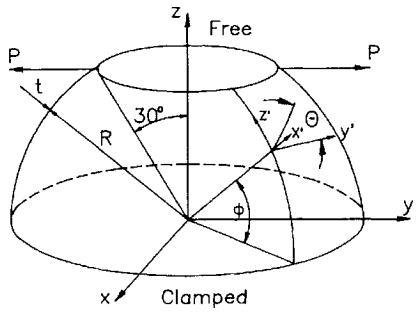

Fig. 3 Clamped hemispherical shell.

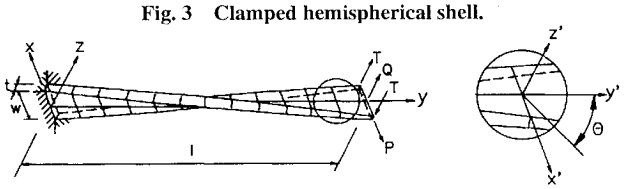

Fig. 4 Pretwisted beam.

the important effect of load condition and unsymmetric arrangement of the plies on the optimum solution.

The geometry is depicted in Fig. 4, and two load cases are considered. The first is a unit couple applied at the beam tip ($P = Q = 0$ and $T = 1$), whereas the second load case ($P = Q = 1$ and $T = 0$) represents a crude first-order approximation of a single rotor blade. The constitutive relationship is defined by $E_{11}/E_{22} = 40$, $E_{22}/G_{12} = \frac{5}{3}$, $E_{22}/G_{13} = \frac{5}{3}$, and $E_{22}/G_{23} = 2$, whereas $\nu_{12} = 0.28$ and $E_{11} = 30 \times 10^6$ psi. The geometric constants are $l = 12$, $w = 1.1$, and $t = 3.2$. The ply layup angle θ (measured in the local x'–y' plane at any point) is shown in Fig. 4. The beam is discretized using an adequately converged[11] 1×6 mesh, and further mesh refinement is not performed.

Table 8 reveals the sensitivity to both load condition and symmetry of arrangement of the plies. For load case 1, either an unsymmetric arrangement of the plies or an increase in the total number of symmetric layers results in a significant reduction of strain energy. For load case 2, neither have a significant effect. Note that optimization under load case 2 was abandoned when a further reduction in strain seemed unreasonable.

Conclusion

Although a fair and direct comparison of different global optimization algorithms is difficult to carry out, this study strongly supports the perception that the SF trajectory approach is very competitive when compared with other existing methods. The multistart trajectory method also has the advantage of having a relatively sound, if somewhat conservative, global stopping criterion where many other methods do not provide any confidence information at all.

The SF-M algorithm, developed here, represents a substantial improvement in efficiency over the original trajectory method. It has proved to be both robust and accurate when applied to test problems and some structural problems of practical interest. Indeed the indications are that the modified algorithm is probably a superior method when problems with either a large number of variables or a very large number of local minima in the region of interest are considered.

The multistart trajectory method remains expensive, but its potential with respect to practical engineering problems is increased by the attractive future possibility of implementing the algorithm on parallel processors, where a number of different trajectories may be generated simultaneously.

References

[1]Schoen, F., "Stochastic Techniques for Global Optimization: A Survey of Recent Advances," *Journal of Global Optimization*, Vol. 1, No. 3, 1991, pp. 207–228.

[2]Törn, A., and Zilinkas, A., *Global Optimization: Lecture Notes in Computer Science*, No. 350, Springer–Verlag, Berlin, 1989.

[3]Snyman, J. A., and Fatti, L. P., "A Multi-Start Global Minimization Algorithm with Dynamic Search Trajectories," *Journal of Optimization Theory and Applications*, Vol. 54, No. 3, 1987, pp. 121–141.

[4]Aluffi-Pentini, F., Parisi, V., and Zirilli, F., "Global Optimization and Stochastic Differential Equations," *Journal of Optimization Theory and Applications*, Vol. 47, No. 1, 1985, pp. 1–16.

[5]Kam, T. Y., and Snyman, J. A., "Optimal Design of Laminated Composite Plates Using a Global Optimization Technique," *Composite Structures*, Vol. 19, No. 4, 1991, pp. 351–370.

[6]El-wakeil, O., and Arora, J. S., "Numerical Experiments with Three Global Optimization Methods," Rept. to General Motors Corp., Optimal Design Lab., Dept. of Civil and Environmental Engineering, Univ. of Iowa, Iowa City, IA, 1991.

[7]Dixon, L. C. W., Gomulka, J., and Hersom, S. E., "Reflections on the Global Optimization Problem," *Optimization in Action*, edited by L. C. W. Dixon, Academic, New York, 1976, pp. 398–435.

[8]Griewank, A. O., "Generalized Descent for Global Optimization," *Journal of Optimization Theory and Applications*, Vol. 34, No. 1, 1981, pp. 11–39.

[9]Groenwold, A. A., and Stander, N., "An Efficient 4-Node 24 d.o.f. Thick Shell Finite Element with 5-Point Quadrature," *Engineering Computations*, Vol. 12, No. 8, 1995, pp. 723–748.

[10]Groenwold, A. A., and Stander, N., "A 24 d.o.f. 4-Node Flat Shell Finite Element for General Unsymmetric Orthotropic Layered Composites," *Engineering Computations* (submitted for publication).

[11]Groenwold, A. A., "Finite Element Analysis of Composite Plates and Shells," M.E. Dissertation, Dept. of Mechanical and Aeronautical Engineering, Univ. of Pretoria, South Africa, 1993.

[12]Tauchert, T. R., and Adibathla, S., "Design of Laminated Plates for Maximum Stiffness," *Journal of Composite Materials*, Vol. 18, No. 1, 1984, pp. 58–69.

[13]Lakshminarayana, H. V., and Murthy, S. S., "A Shear Flexible Triangular Finite Element Model for Laminated Composite Plates," *International Journal for Numerical Methods in Engineering*, Vol. 20, No. 4, 1984, pp. 591–623.

[14]Moser, K., and Schmid, A., "Composite Structures—Modeling, Finite Element Analysis and Evaluation," *Composite Structures*, Vol. 11, No. 1, 1989, pp. 33–56.